Available online at www.sciencedirect.com
ScienceDirect
Dyes and Pigments 75 (2007) 434–442
DYES and PIGMENTS
www.elsevier.com/locate/dyepig

Photocatalyzed *N*-de-methylation and degradation of crystal violet in titania dispersions under UV irradiation

Chiing-Chang Chen [a], Fu-Der Mai [b], Kung-Tung Chen [c], Chia-Wei Wu [b], Chung-Shin Lu [a,*]

[a] *Department of General Education, National Taichung Nursing College, Taichung 403, Taiwan, ROC*
[b] *Department of Applied Chemistry, Chung-Shan Medical University, Taichung 402, Taiwan, ROC*
[c] *Department of General Education, Ming Hsin University of Science and Technology, Hsin-Chu 304, Taiwan, ROC*

Received 12 November 2005; received in revised form 22 January 2006; accepted 16 June 2006
Available online 25 September 2006

Abstract

TiO_2-mediated photocatalytic process has been successfully applied to degrade dye pollutants. In order to obtain a better understanding on the mechanistic details of the TiO_2-assisted photodegradation of crystal violet (CV, *N*,*N*,*N*′,*N*′,*N*″,*N*″-hexamethylpararosaniline) dye with UV irradiation, 17 intermediates of the process were separated, identified and characterized by HPLC–ESI-MS techniques in this study. The results indicated that the *N*-de-methylation degradation of CV dye took place in a stepwise manner to yield mono-, di-, tri-, tetra-, penta-, and hexa-*N*-de-methylated CV species with *N*-hydroxymethylated intermediates, which were found for the first time, generated during the processes. Several probable photodegradation pathways were proposed and discussed. The reaction mechanisms of TiO_2/UV proposed in this study would be useful for future application of this technology for decoloration of dyes.

Keywords: Crystal violet; Dye; Photodegradation; TiO_2; *N*-De-methylation

1. Introduction

It is reported that 10–20% of dyes are lost in wastewater as a result of inefficiency in the dyeing process [1]. Dyestuffs from the textile and photographic industries are becoming a major source of environmental pollution. The large amount of dyestuffs used in the dyeing stage of textile manufacturing processes represents an increasing environmental danger due to their refractory carcinogenic nature [2,3]. To de-pollute the dyeing wastewater, a number of methods have been investigated including chemical oxidation and reduction, chemical precipitation and flocculation, photolysis, adsorption, ion pair extraction, electrochemical treatment and advanced oxidation [4,5].

The advanced oxidation technology is one of the promising technologies for the removal of dye-contaminated wastewaters due to its high efficiency. This technology is mainly based on the oxidative reactivity of $HO^{\bullet}$ radicals generated by various methods such as O_3/UV, H_2O_2/UV, H_2O_2/vis, O_3/H_2O_2/UV photolysis, photoassisted Fe^{3+}/H_2O_2, and TiO_2-mediated photocatalytic processes.

TiO_2-mediated photocatalytic process has been successfully applied to degrade pollutants during the past few years [6–17]. TiO_2 is broadly used as a photocatalyst because of its nontoxicity, photochemical stability and low cost [18–21]. The initial step in the TiO_2-mediated photocatalytic degradation is proposed to involve the generation of e^-/h^+ pair leading to the formation of hydroxyl radicals ($^{\bullet}OH$), superoxide radical anions ($O_2^{\bullet-}$) and hydroperoxyl radicals ($^{\bullet}OOH$) and these radicals are the oxidizing species in the photocatalytic oxidation processes. The efficiency of dye degradation depends on the concentration of the oxygen molecules, which either scavenge the conduction band electrons (e_{cb}^-) or prevent the recombination of e^-/h^+. The electron in the conduction band can be picked up by the adsorbed dye molecules, leading to the formation of dye radical anions and the degradation of dye [21].

* Corresponding author. Tel.: +886 4 2219 6973; fax: +886 4 2219 4990.
E-mail address: ccchen@ntcnc.edu.tw (C.-S. Lu).

0143-7208/$ - see front matter © 2006 Elsevier Ltd. All rights reserved.
doi:10.1016/j.dyepig.2006.06.040

Triphenylmethane dyes are used extensively in textile industry for dyeing nylon, wool, cotton, and silk, as well as for coloring of oil, fats, waxes, varnish, and plastics. Paper, leather, cosmetic, and food industries consume a high quantity of triphenylmethane dyes in various kinds [1,22,23]. Additionally, the triphenylmethane dyes are applied as staining agents in bacteriological and histopathological applications [24]. The photocytotoxicity of triphenylmethane dyes, based on the production of the reactive oxygen species, is tested intensively with the regard of their photodynamic treatment [25–30]. However, there is a great concern about the thyroid peroxidase-catalyzed oxidation of the triphenylmethane class of dyes because the reactions might form various *N*-de-alkylated primary and secondary aromatic amines, whose structures are similar to aromatic amine carcinogens [31,32].

It has been reported that crystal violet appears to photodegrade via two competitive pathways: (i) *N*-de-methylation of the chromophore skeleton, and (ii) cleavage of the whole conjugated chromophore structure [33,34]. The *N*-de-methylation process was presumed to exist on the basis of the wavelength shift of maximal absorption of the dyes. However, the *N*-de-methylation intermediates of CV dyes have not been isolated and identified by HPLC–ESI-MS techniques. The mechanistic details of the *N*-de-methylated process and cleavage of the whole conjugated chromophore structure still remain uncertain.

Accordingly, this study focused on the identification of the *N*-de-methylation reaction intermediates and shed some light on the mechanistic details of photodegradation of CV dye in the TiO_2/UV process, which in turn can serve as foundation for future application.

2. Experimental section

2.1. Materials

The TiO_2 nanoparticle (P25, ca. 80% anatase, 20% rutile; particle size, ca. 20–30 nm; BET area, ca. 55 $m^2\,g^{-1}$) was supplied by Degussa Co. CV dye was obtained from Tokyo Kasei Kogyo Co. and used without any further purification. Chemical structure of the CV dye is shown in Fig. 1. Stock solutions containing 1 $g\,L^{-1}$ of CV dye in water were prepared, protected from light, and stored at 4 °C. HPLC analysis was employed to confirm the presence of the CV dye as a pure organic compound.

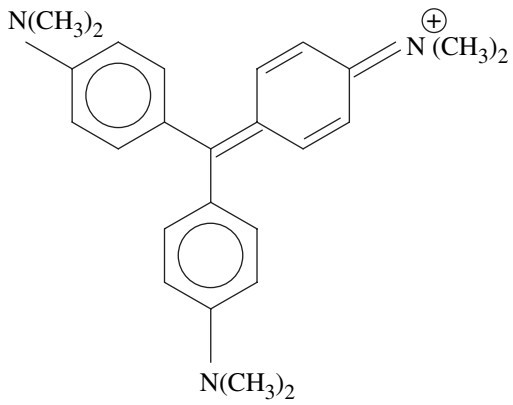

Fig. 1. Chemical structure of crystal violet.

Reagent-grade ammonium acetate, sodium hydroxide, nitric acid and HPLC-grade methanol were purchased from Merck. De-ionized water was used throughout this study. The water was then purified with a Milli-Q water ion-exchange system (Millipore Co.) to give a resistivity of $1.8 \times 10^7\ \Omega\,cm$.

2.2. Instruments

Waters ZQ LC/MS system, equipped with a binary pump, a photodiode array detector, an autosampler and a micromass detector, was used for separation and identification. The C-75 Chromato-Vue cabinet of UVP provides a wide area of illumination from the 15-W UV-365 nm tubes positioned on two sides of the cabinet interior.

2.3. Procedure and analysis

An aqueous TiO_2 dispersion was prepared by adding 50 mg of TiO_2 powder to a 100 mL solution containing the CV dye at appropriate concentrations. For reactions in different pH media, the initial pH of the suspensions was adjusted by addition of either NaOH or HNO_3 solutions. Prior to irradiation, the dispersions were magnetically stirred in the dark for ca. 30 min to ensure the establishment of an adsorption/desorption equilibrium. Irradiations were carried out using two UV-365 nm lamps (15 W). At any given irradiation time interval, the dispersion was sampled (5 mL), centrifuged, and subsequently filtered through a Millipore filter (pore size, 0.22 μm) to separate the TiO_2 particles.

After each irradiation cycle, the amount of the residual dye was thus determined by HPLC. The analysis of organic intermediates was accomplished by HPLC–ESI-MS techniques after the readjustment of the chromatographic conditions in order to make the mobile phase compatible with the working conditions of the mass spectrometer. Two different kinds of solvents were prepared in this study. Solvent A was 25 mM aqueous ammonium acetate buffer (pH 6.9), while solvent B was methanol instead of ammonium acetate. LC was carried out on an Atlantis™ dC18 column (250 mm × 4.6 mm i.d., diameter particle (dp) = 5 μm). The flow rate of the mobile phase was set to be 1.0 mL/min. A linear gradient was set as follows: $t = 0$, $A = 95$, $B = 5$; $t = 20$, $A = 50$, $B = 50$; $t = 40$–45, $A = 10$, $B = 90$; $t = 48$, $A = 95$, $B = 5$. The column effluent was introduced into the ESI source of the mass spectrometer. Equipped with an ESI interface, the quadruple mass spectrometer with heated nebulizer probe at 350 °C was used with an ion source temperature of 80 °C. ESI was carried out with the vaporizer at 350 °C and nitrogen as sheath (80 psi) and auxiliary (20 psi) gas to assist the preliminary nebulization and to initiate the ionization process. A discharge current of 5 μA was applied. Tube lens and capillary voltages were optimized for the maximum response during perfusion of CV standard.

Performed in flask without addition of TiO_2, the blank experiments show no appreciable decolorization of the irradiated solution, thus confirmed the expected stability of this CV dye under UV light irradiation. Also with addition of 0.5 g L^{-1} TiO_2 to solutions, which contain 50 mg L^{-1} of the CV dye, the stability of the dye did not alter in the dark either.

3. Results and discussion

3.1. pH effect

In an aqueous system, TiO_2 is amphoteric [35]. The TiO_2 surface is predominantly negatively charged when the pH is higher than the isoelectric point of TiO_2. As the pH decreases, the functional groups are protonated and the proportion of the positively charged surface increases. Thus, the electrical property of the TiO_2 surface varies with the pH of the dispersion [36]. The surface of TiO_2 would be negatively charged and would adsorb cationic species easily under $pH > pI$ conditions; while in the reverse condition it would adsorb anionic ones. However, the adsorption of the substrate onto the TiO_2 surface directly affects the occurrence of electron transfer between the excited dye and TiO_2 and further influences the degradation rate. The surface becomes positively charged, and the number of adsorption sites may decrease above the isoelectric point of TiO_2. A similar effect of pH on the adsorption and photocatalytic reaction has been reported for Ag deposition [37] and the degradation of formic acid [38].

The photodegradation rate of the CV dye as a function of reaction pH is shown in Fig. 2. The photodegradation rate of the CV dye was found to increase with the increase in the value of pH. Under an acidic condition, it was found that the cationic CV dye was difficult to adsorb onto the TiO_2 surface, usually with the active $^{\bullet}OH$ radicals, formed in low concentration, and hence the photodegradation process of CV remained very slow. With higher pH values, the formation of active $^{\bullet}OH$ species is favored, due to not only improved transfer of holes to the adsorbed hydroxyls, but also electrostatic abstractive effects between the negatively charged TiO_2 particles and the operating cationic dyes. Although the CV dye can adsorb onto the TiO_2 surface to some extent in alkaline media, however, when the pH value is too high (pH = 11), the CV dye molecules will change to a leuco compound. In a good agreement with the adsorption mechanism proposed in Ref. [34], our results indicate that the TiO_2 surface is negatively charged and the CV adsorbs onto the TiO_2 surface through the positive ammonium groups.

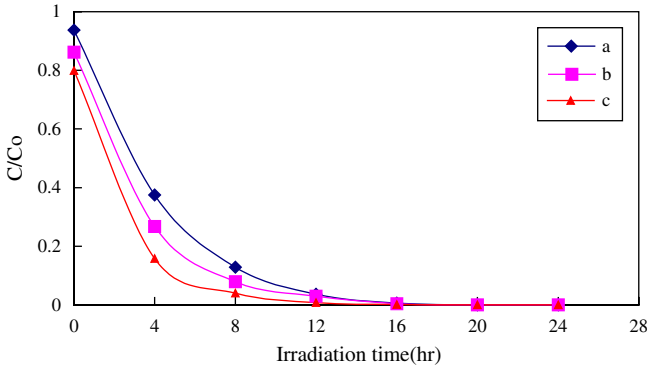

Fig. 2. pH effect on the CV photodegradation rate with concentrations of TiO_2 being 0.5 g L^{-1} and CV being 0.05 g L^{-1}: (a) pH 5; (b) pH 6; (c) pH 9.

3.2. Effect of photocatalyst concentration

It is important from both the mechanistic and applicational points of view to study the dependence of the photocatalytic reaction rate on the concentration of TiO_2 in the CV dye. Hence, the effect of photocatalyst concentration on the photodegradation rate of the CV dye was investigated by employing different concentrations of TiO_2 varying from 0.1 to 0.5 g L^{-1}. As expected, the photodegradation rate of CV was found to increase with the increase in the catalyst concentration (Fig. 3), a general characteristic of heterogeneous photocatalyst, and our results are in agreement with the earlier reports [33]. It is known, however, that there exists a practical limit of the scattering light (around 1 g L^{-1}), above which the degradation rate will decrease due to the reduction of the photonic flux within the irradiated solution.

3.3. UV–vis spectra

The aqueous solution of the CV dye was fairly stable under UV radiation in absence of TiO_2. However, the CV dye can be degraded efficiently in aqueous CV/TiO_2 dispersions by UV irradiation at wavelength 365 nm. The changes of the UV–vis spectra during the photodegradation process of the CV dye in the aqueous TiO_2 dispersions under UV irradiation are illustrated in Fig. 4. After UV irradiation for 16 h, ca. 99.5% of the CV dye was degraded. During UV irradiation, the characteristic absorption band of the dye around 588.3 nm decreased rapidly with slight hypsochromic shifts (555.4 nm), but no new absorption bands appeared even in

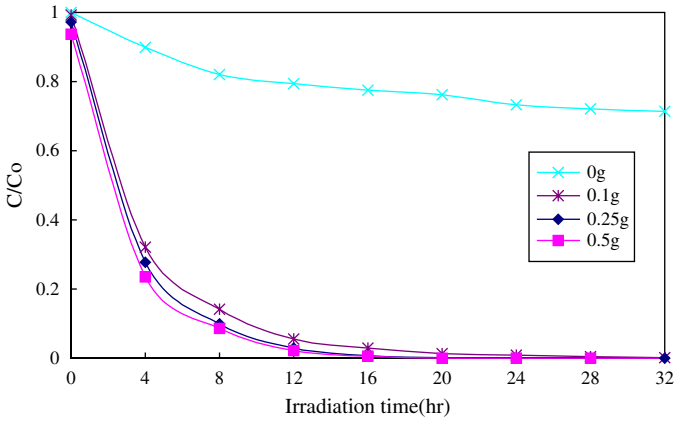

Fig. 3. Influence of the catalyst concentration on the photodegradation rate for the decomposition of CV. Experimental condition: dye concentration (0.05 g L^{-1}), $V = 100$ mL, flask photoreactor, two 15 W Hg lamps, P25 (0, 0.1, 0.25 and 0.5 g L^{-1}), absorbance recorded at 580 nm, continuous stirring, and irradiation time being 32 h.

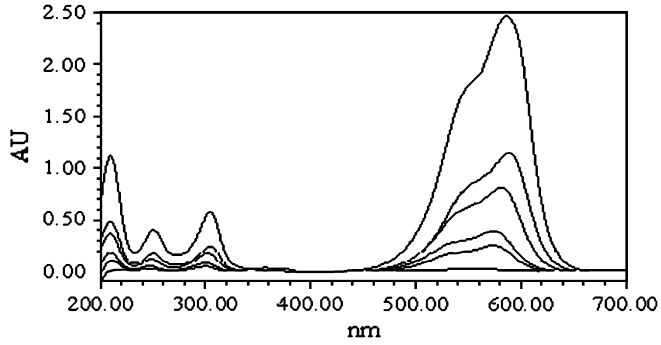

Fig. 4. UV–vis spectral changes of the CV dye in aqueous TiO_2 dispersions (CV, 0.05 g L^{-1}; TiO_2, 0.5 g L^{-1}; pH 6) as a function of the irradiation time. Spectra from top to bottom correspond to the irradiation times of 0, 4, 8, 12, 16, and 24 h, respectively.

ultraviolet range ($\lambda > 200$ nm), which indicated that there might be formation of a series of *N*-de-methylated intermediates and cleavage of the whole conjugated chromophore structure of the CV dye. Further irradiation caused the decrease of the absorption band at 555.4 nm, but no further wavelength shift was observed, inferring that the band at 555.4 nm is that of the full *N*-de-methylated product of the CV dye.

3.4. Separation and identification of the intermediates

Temporal variations occurring in the solution of the CV dye during the photodegradation process with UV irradiation were examined with HPLC, coupled with a photodiode array detector, and ESI mass spectrometry. The relevant change in the chromatograms recorded at 580 nm is illustrated in Fig. 5. With irradiation up to 24 h, 17 components are identified all with the retention time less than 50 min. We denoted the CV dye and its related intermediates as species **A**–**J**, **A′**–**E′**, **B″** and **C″** (see Table 1 for detail). Except for the initial CV dye (peak **A**), the intensities of other peaks increased at first and subsequently decreased, indicating the formation and transformation of the intermediates. The absorption spectra of each intermediate in the visible spectral region are depicted in Fig. 6; they are identified as **A**–**J** (Fig. 6a) and **A′**–**E′** (Fig. 6b), corresponding to the peaks **A**–**J** and **A′**–**E′** in Fig. 5, respectively. The absorption maximum of the spectral bands shifts hypsochromically from 588.3 (Fig. 6a, spectrum A) to 555.4 nm (Fig. 6a, spectrum J) and 609.1 (Fig. 6b, spectrum A′) to 581.4 nm (Fig. 6b, spectrum E′). This hypsochromic shift of the absorption band is presumed to result from the formation of series of *N*-de-methylated intermediates in a stepwise manner. Further irradiation caused the decrease of the absorption band at 555.4 nm, but no further wavelength shift was observed, inferring that the band at 555.4 nm is that of the full *N*-de-methylated product of CV dye. Similar phenomena were also observed during the photodegradation of rhodamine-B [39,40] and sulforhodamine-B [7,41] under visible irradiation. Moreover, in Fig. 6b, the hypsochromic shift of the absorption band is surmised as the result of series of *N*-hydroxymethylated intermediates formed in a stepwise manner.

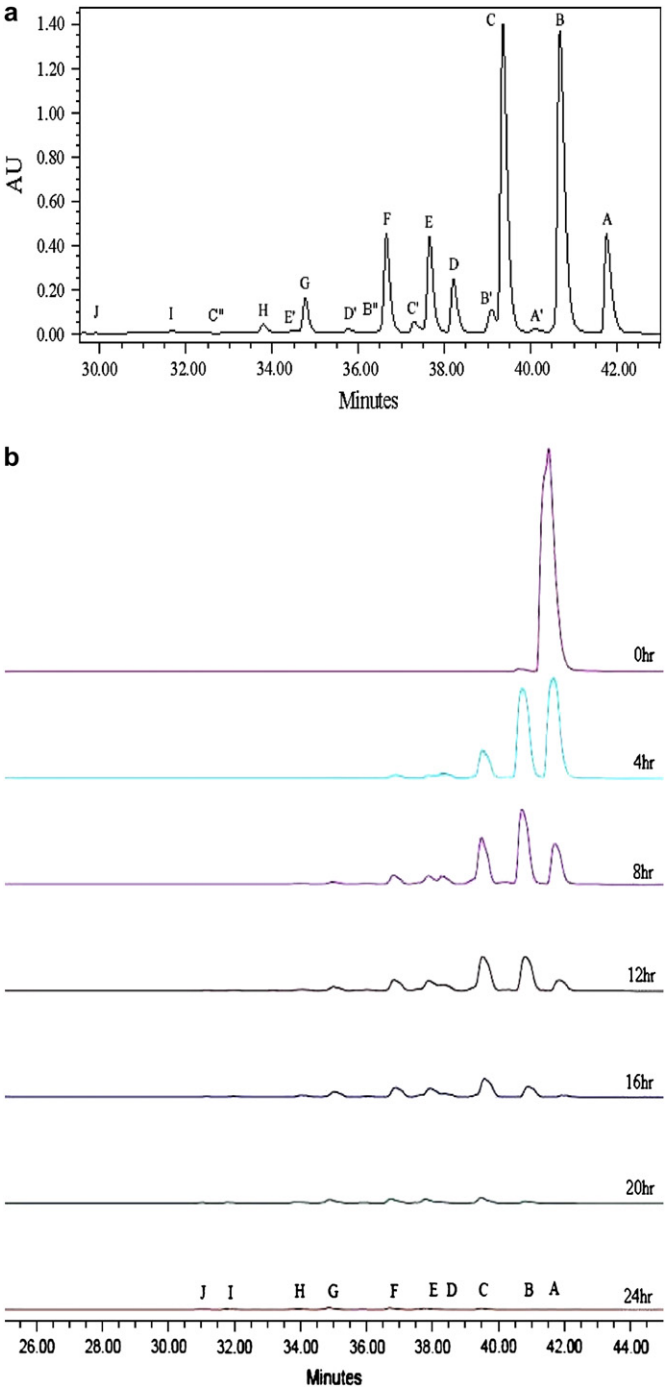

Fig. 5. (a) HPLC chromatogram of the *N*-de-methylated intermediates with 12 h of irradiation, recorded at 580 nm. (b) HPLC chromatogram of the *N*-de-methylated intermediates at different irradiation intervals, recorded at 580 nm. Spectra from top to bottom correspond to the irradiation times of 0, 4, 8, 12, 16, 20, and 24 h, respectively.

As depicted in Fig. 6, the wavelength shifts are due to the *N*-de-methylation of the CV dye caused by the attacks of some active oxygen species on the *N*,*N*-dimethyl and *N*-methyl groups. Examination of the spectral variation of Fig. 4 and temporal behavior of Fig. 5b suggests that the CV dye is *N*-de-methylated in a stepwise manner (i.e., methyl groups are removed one by one as confirmed by the gradual

Table 1
Identification of the *N*-de-methylation intermediates of the CV dye by HPLC–ESI-MS

HPLC peaks	*N*-De-methylation intermediates	Abbreviation	ESI–MS peaks (*m/z*)	Absorption maximum (nm)
A	*N*,*N*,*N*′,*N*′,*N*″,*N*″-Hexamethylpararosaniline	CV	372.18	588.3
B	*N*,*N*-Dimethyl-*N*′,*N*′-dimethyl-*N*″-methylpararosaniline	DDMPR	358.14	581.0
C	*N*,*N*-Dimethyl-*N*′-methyl-*N*″-methylpararosaniline	DMMPR	344.15	573.7
D	*N*,*N*-Dimethyl-*N*′,*N*′-dimethylpararosaniline	DDPR	344.15	579.8
E	*N*-Methyl-*N*′-methyl-*N*″-methylpararosaniline	MMMPR	330.16	566.3
F	*N*,*N*-Dimethyl-*N*′-methylpararosaniline	DMPR	330.16	570.0
G	*N*-Methyl-*N*′-methylpararosaniline	MMPR	316.18	562.7
H	*N*,*N*-Dimethylpararosaniline	DPR	316.11	567.6
I	*N*-Methylpararosaniline	MPR	302.06	561.5
J	Pararosaniline	PR	288.07	555.4
A′	*N*,*N*-Dimethyl-*N*′,*N*′-dimethyl-*N*″-hydroxymethyl-*N*″-methylpararosaniline	DDHMPR	388.12	609.1
B′	*N*,*N*-Dimethyl-*N*′-hydroxymethyl-*N*′-methyl-*N*″-methylpararosaniline	DHMMPR	374.14	593.3
B″	*N*,*N*-Dimethyl-*N*′,*N*′-methyl-*N*″-hydroxymethylpararosaniline	DDHPR	374.20	596.9
C′	*N*-Hydroxymethyl-*N*-methyl-*N*′-methyl-*N*″-methylpararosaniline	HMMMPR	360.15	582.2
C″	*N*,*N*-Dimethyl-*N*′-methyl-*N*″-hydroxymethylpararosaniline	DMHPR	360.21	583.4
D′	*N*,*N*-Dimethyl-*N*′-hydroxymethyl-*N*′-methylpararosaniline	DHMPR	360.16	584.7
E′	*N*-Methyl-*N*′-methyl-*N*″-hydroxymethylpararosaniline	MMHPR	346.04	581.4

peak wavelength shifts toward the blue region). The wavelength of the major absorption peaks for the *N*-de-methylated CV products are all found with blue shift with respect to that of CV. The results are summarized in Table 1. During the initial period of photodegradation of the CV dye, competitive reactions between *N*-de-methylation and cleavage of the CV chromophore ring structure occur, however, with *N*-de-methylation being predominant.

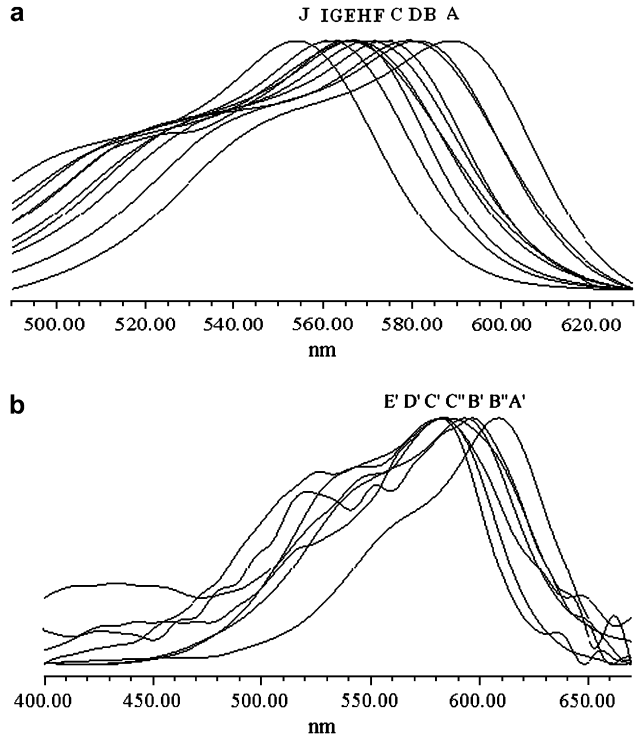

Fig. 6. Absorption spectra of the *N*-de-methylated intermediates formed during the photodegradation process of the CV dye corresponding to the peaks in the HPLC chromatograph of Fig. 3. Spectra were recorded using the photodiode array detector. Spectra A–J and A′–E′ correspond to the peaks A–J and A′–E′, respectively, in Fig. 5.

The *N*-de-methylated intermediates were further identified using HPLC–ESI-MS techniques; the relevant mass spectra are illustrated in Fig. 7. The molecular ion peaks appeared to be in the acid forms of the intermediates. From the results of mass spectral analysis, we confirmed that component **A**, $m/z = 372.18$, (Fig. 7, mass spectra A); the other components are **B**, $m/z = 358.14$, *N*,*N*-dimethyl-*N*′,*N*′-dimethyl-*N*″-methylpararosaniline (Fig. 7, mass spectra B); **C**, $m/z = 344.15$, *N*,*N*-dimethyl-*N*′-methyl-*N*″-methylpararosaniline (Fig. 7, mass spectra C); **D**, $m/z = 344.15$, *N*-methyl-*N*′,*N*′-dimethylpararosaniline (Fig. 7, mass spectra D); **E**, $m/z = 330.16$, *N*-methyl-*N*′-methyl-*N*″-methylpararosaniline (Fig. 7, mass spectra E); **F**, $m/z = 330.16$, *N*,*N*-dimethyl-*N*′-methylpararosaniline (Fig. 7, mass spectra F); **G**, $m/z = 316.18$, *N*-methyl-*N*′-methylpararosaniline (Fig. 7, mass spectra G); **H**, $m/z = 316.11$, *N*,*N*-dimethylpararosaniline (Fig. 7, mass spectra H); **I**, $m/z = 302.06$, *N*-methylpararosaniline (Fig. 7, mass spectra I); **J**, $m/z = 288.07$, pararosaniline (Fig. 7, mass spectra J); **A**′, $m/z = 388.12$, *N*,*N*-dimethyl-*N*′,*N*′-dimethyl-*N*″-hydroxymethyl-*N*″-methylpararosaniline (Fig. 7, mass spectra A′); **B**′, $m/z = 374.14$, *N*,*N*-dimethyl-*N*′-hydroxymethyl-*N*′-methyl-*N*″-methylpararosaniline (Fig. 7, mass spectra B′); **B**″, $m/z = 374.20$, *N*,*N*-dimethyl-*N*′,*N*′-dimethyl-*N*″-hydroxymethylpararosaniline (Fig. 7, mass spectra B″); **C**′, $m/z = 360.15$, *N*-hydroxymethyl-*N*-methyl-*N*′-methyl-*N*″-methylpararosaniline (Fig. 7, mass spectra C′); **C**″, $m/z = 360.21$, *N*,*N*-dimethyl-*N*′-methyl-*N*″-hydroxymethylpararosaniline (Fig. 7, mass spectra C″); **D**′, $m/z = 346.16$, *N*,*N*-dimethyl-*N*′-hydroxymethyl-*N*′-methylpararosaniline (Fig. 7, mass spectra D′); **E**′, $m/z = 346.12$, *N*-methyl-*N*′-methyl-*N*″-hydroxymethylpararosaniline (Fig. 7, mass spectra E′). Results of HPLC chromatograms, UV–vis spectra, and mass spectra are summarized in the Table 1.

It is interesting to note that peak D emerged prior to peak C and peak F emerged prior to peak E (Fig. 5b). However, unlike other peaks, the absorption maximum of intermediate **D** (579.8 nm) occurs at a longer wavelength than that of

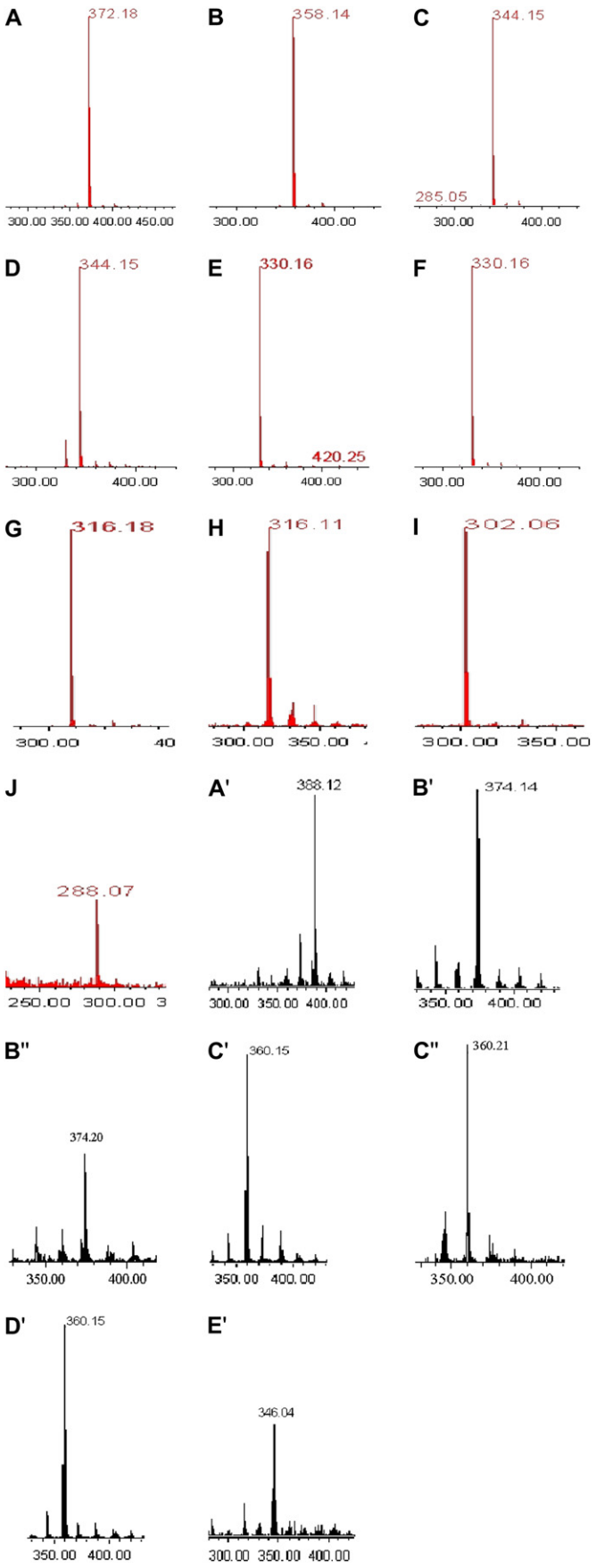

intermediate **C** (573.7 nm); the absorption maximum of intermediate **F** (570.0 nm) occurs at a longer wavelength than that of intermediate **E** (566.3 nm); the absorption maximum of intermediate **H** (567.6 nm) occurs at a longer wavelength than that of intermediate **G** (562.7 nm). However, the emerging intermediates whose absorption-maximum peaks cannot be easily observed in Fig. 5b, but can be observed in Fig. 8, are corresponding to those species with several methyl groups detached from the CV dye. According to the number of the methyl groups detached, we can characterize these intermediates. We have found that there exist three different pairs of isomeric molecules, i.e., di-, tri-, and tetra-*N*-de-methylated CV species, differing only by the way in loosing the methyl groups from the benzyl groups. One of the di-*N*-de-methylated CV isomers, DMMPR, is formed by the removal of a methyl group from two different benzyl groups of the CV molecule, whereas the other isomer, DDPR, is produced by loosing two methyl groups from the same benzyl group of the CV dye. In the tri-*N*-de-methylated CV isomers, MMMPR, is formed by the removal of one methyl group from every benzyl group of the CV molecule, whereas the other isomer in this pair, DMPR, is produced by removing two methyl groups from the same benzyl group of the CV and the removal of the third methyl group from another benzyl group of the CV dye. In the last pair of isomers, DPR, is formed by removing two methyl groups from each of the two methyl groups in the CV molecule, whereas the other isomer in this pair, MMPR, is produced by first abstracting two methyl groups from the same benzyl group of the CV and removing one methyl group from each of the remaining two benzyl groups in the CV dye. Therefore, considering the polarity of the DDPR, DMPR and DPR species is greater than that of the DMMPR, MMMPR and MMPR intermediates, and we expected the latter to be eluted after the DDPR, DMPR and DPR species. As well, since the two *N*-methyl groups are stronger auxochromic moieties than the *N*,*N*-dimethyl groups and amino group, the maximal absorption of the DDPR, DMPR and DPR intermediates was anticipated to occur at wavelengths shorter than the band position of the DMMPR, MMMPR and MMPR species. In the previous report [42], the formation of *N*-methylamino moiety by the ozone attack of *N*,*N*-dimethylamino group can be explained by the initial electrophilic attack of ozone at the nitrogen atom. With the identical intermediates, the hydroxymethylamino derivatives can also be obtained by a similar manner. The intermediates, **A′**–**E′**, **B″** and **C″**, are generated by *N*-de-methylation of the CV dye due to the attack by one of the active oxygen species on the *N*,*N*-dimethyl or *N*-methyl groups produced the hydroxymethylamino derivatives. Similarly, since the *N*-hydroxymethyl groups are weaker auxochromic moieties than the *N*,*N*-dimethyl or *N*-methyl groups, the maximal absorption of the **A′**–**E′**, **B″** and **C″** intermediates was anticipated to occur at wavelengths longer

Fig. 7. ESI mass spectra of *N*-de-methylated intermediates formed during the photodegradation of the CV dye after they were separated by HPLC method: mass spectra denoting **A**–**J** and **A′**–**E′** correspond to the **A**–**J** and **A′**–**E′** species in Fig. 5, respectively.

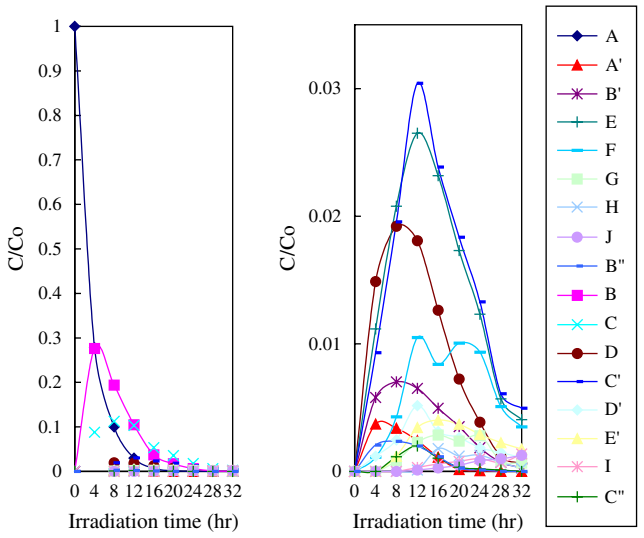

Fig. 8. Variation in the relative distribution of the *N*-de-methylated products obtained from the photodegradation of the CV dye as a function of the irradiation time. Curves A–J correspond to the peaks A–J in Fig. 5, respectively.

than the band position of the **A–J** species, respectively. This argument will be supported by the following results and a mechanism is proposed accordingly.

The relative distribution of the *N*-de-methylated intermediates obtained is illustrated in Fig. 8. To minimize errors, the relative intensities were recorded at the maximum absorption wavelength for each intermediate, although a complete quantitative determination of all of the photogenerated intermediates was not achieved, owing to the lack of the appropriate molar extinction coefficients of these intermediates and the related reference standards. Nonetheless, we clearly observed the changes in the distribution of each intermediate during the photodegradation process of the CV dye. In accordance with the data of Fig. 5b, the successive appearance of the maximal distribution of each intermediate indicates that the *N*-de-methylation of CV is a stepwise photochemical process.

Under UV irradiation, most of the $^{\bullet}OH$ radicals are generated directly from the reaction between the holes and surface-adsorbed H_2O or OH^-. The probability for the formation of $O_2^{-\bullet}$ should be much less than that of $^{\bullet}OH$ [39]. The *N*-de-methylation of the CV dye occurs mostly by the attack of the $^{\bullet}OH$ species on the *N*,*N*-dimethyl groups of the CV dye. Considering that the *N*,*N*-dimethyl group in DDPR, DMPR and DPR is bulkier than the *N*-methyl group in DMMPR, MMMPR and MMPR molecules, the attack of $^{\bullet}OH$ radicals on the *N*-methyl groups should be favored at the expense of *N*,*N*-dimethyl groups. In accordance with this notion, the HPLC results showed that the DDPR, DMPR, and DPR intermediates reached maximal concentration before the DMMPR, MMMPR, and MMPR intermediates did. But considering that the probability of the two *N*,*N*-dimethyl groups in DDMPR is higher than in the one *N*-methyl group in DDMPR molecules, the attack by $^{\bullet}OH$ on the *N*,*N*-dimethyl group should be favored over the *N*-methyl group. The *N*-di-de-methylated intermediates (DMMPR and DDPR) were clearly observed (Fig. 8, curves C and D), in that DMMPR and DDPR reached its maximum concentration after 12- and 8-h irradiation periods due to the two competitive factors as mentioned above. The *N*-tri-de-methylated intermediates (MMMPR and DMPR) were clearly observed (Fig. 8, curves E and F), in that MMMPR reached its maximum concentration after a 12-h irradiation period, while DMPR reached two maximum concentrations after 12- and 20-h because the $^{\bullet}OH$ attacked the *N*-methyl groups of DMMPR and *N*,*N*-dimethyl group of DDPR. The *N*-tetra-de-methylated intermediates (MMPR and DPR) were clearly observed (Fig. 8, curves G and H) in that MMPR reached its maximum concentration after a 16- and 24-h irradiation periods because the $^{\bullet}OH$ attacked *N*-methyl group of MMMPR and *N*,*N*-dimethyl group of DMPR, while DPR reached its two maximum concentrations after 16- and 24-h irradiation periods because DMPR produced by DMMPR and DDPR reached its two maximum concentrations in different irradiation times. In the *N*-penta-de-methylated intermediates (MPR) (Fig. 8, curve I), MPR reached its maximum concentration after 24- and 32-h irradiation periods because the $^{\bullet}OH$ attacked *N*-methyl group of MMPR and *N*,*N*-dimethyl group of DPR. In the *N*-hexa-de-methylated intermediates (PR) (Fig. 8, curve J), PR reached its maximum concentration after a 32-h irradiation period.

In the hydroxylation of the *N*-hexa-methylated intermediate (Fig. 8, curve A′), DDHMPR reached its maximum concentration after a 4-h irradiation period because the $^{\bullet}OH$ attacked *N*,*N*-dimethyl group of CV. In the hydroxylation of the *N*-penta-methylated intermediates (Fig. 6, curves B′ and B″), DHMMPR and DDHPR reached their maximum concentrations after an 8-h irradiation period because the $^{\bullet}OH$ attacked *N*,*N*-dimethyl group of DDMPR and *N*-methyl group of DDMPR. In the hydroxylation of *N*-tetra-methylated intermediates (Fig. 8, curves C′ and C″), HMMMPR and DMHPR reached their maximum concentrations after a 12-h irradiation period because the $^{\bullet}OH$ attacked *N*,*N*-dimethyl group of DMMPR and *N*-methyl group of DMMPR. In the hydroxylation of *N*-tetra-methylated intermediates (Fig. 8, curve D′), DHMPR reached its maximum concentration after a 12-h irradiation period because the $^{\bullet}OH$ attacked *N*,*N*-methyl group of DDPR. In the hydroxylation of *N*-tri-methylated intermediate (Fig. 8, curve E′), MMHPR reached its maximum concentration after a 16-h irradiation period because the $^{\bullet}OH$ attacked *N*-methyl group of MMMPR. The successive appearance of the maximal quantity of each intermediate indicates that the *N*-de-methylation of CV is a stepwise photochemical process by de-hydroxylation of *N*-hydroxymethylated intermediates. The results we discussed is depicted more clearly in Scheme 1.

The *N*-mono-de-methylated intermediates (PPR) and *N*-di-de-methylated intermediates (DDPR and DMMPR) were clearly observed (Fig. 8, curves B–D), following which PPR degraded rapidly. A small amount of the sixth *N*-de-methylated intermediate (PR) was also detected (Fig. 8, curve J). The first product (DDMPR) of *N*-de-methylation reached its maximum concentration after a 4-h irradiation period (Fig. 8, curve B), whereas the maximum of the full *N*-de-methylated product (PR) appeared after 32-h irradiation (Fig. 8, curve J). The chromophoric species (CV) was still observed

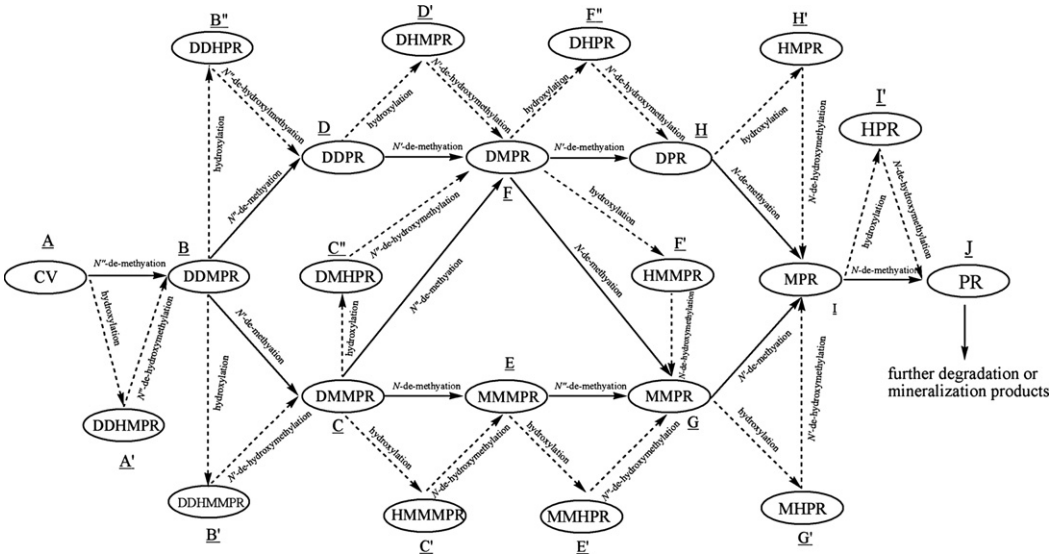

Scheme 1. Proposed photodegradation mechanism of the CV dye under UV irradiation in aqueous TiO_2 dispersions followed by the identification of several intermediates by HPLC–ESI mass spectral techniques.

even after irradiation for 32 h. This indicates that the *N*-de-methylation process by hydroxylation predominates and the cleavage of the conjugated structure occurs at a somewhat slower rate until all the six methyl groups are removed.

When the CV dye molecules are located near the TiO_2 surface due to the dimethylamine group, which somewhat neutralizes the surface, the *N*-de-methylation process predominates during the initial stages. Destruction of the chromophore ring structure occurs mostly only after full de-methylation of the dye appears.

According to earlier reports [43–45], most oxidative *N*-de-alkylation processes are preceded by the formation of nitrogen-centered radical, whereas the destruction of the dye chromophore structures is preceded by the generation of the carbon-centered radical [34,40,46–48]. To be consistent with the above statement, the degradation of CV must occur via two different photooxidation pathways (destruction of the chromophore structure and *N*-de-methylation) due to the formation of the different radicals (either carbon-centered radical or nitrogen-centered radical). There is no doubt that electron injection from the dye to the conduction band of TiO_2 yields the dye cation radical, a process which is determined by the nature of the HOMO orbital of the excited dye ^{1,3}dye* [41]. After this stage, the cation radical, dye$^{\bullet+}$, can undergo hydrolysis and/or de-protonation pathways of the dye cation radicals, which in turn are determined by the different adsorption modes of CV on the TiO_2 particle surface.

On the basis of all the above experimental results, we tentatively propose the pathway of de-methylation as depicted in Scheme 1. The dye molecule in the CV/TiO_2 system is adsorbed through the positively charged dimethylamine groups. Then the electrons are injected from the TiO_2 particle surface to the adsorbed dye through the positively charged dimethylamine groups and the subsequence hydrolysis (or de-protonation) yields a nitrogen-centered radical, which is then attacked by molecular oxygen to lead ultimately to de-methylation. The mono-de-methylated dye derivative, DDMPR, can also be adsorbed on TiO_2 particle surface and be involved in other similar events (such as electron injection, oxygen attack and hydrolysis or de-protonation) to yield a bi-de-methylated dye derivative, DDPR and DMMPR. The de-methylation process, as described above, continues until formation of the completely de-methylated dye, PR.

4. Conclusion

The CV dye could be successfully decolorized and degraded by TiO_2 under UV irradiation. Both *N*-de-methylation and degradation of the CV dye take place in presence of TiO_2 particles. The photodegradation rate of the CV dye was found to increase along with the increase in both the value of pH and the catalyst concentration. After 15 W UV-365 nm irradiation for 16 h, ca. 99.5% of CV was degraded. In TiO_2-assisted photodegradation of triphenylmethane dye, the *N*-de-alkylation process predominates by the hydroxylated intermediates during the initial irradiation period, as found and identified by HPLC–ESI-MS and UV–vis spectra for the first time. The *N*-de-methylation of the CV dye takes place in a stepwise manner with the various *N*-de-methylated and hydroxylated intermediate CV species. The *N*-de-methylation process continues until the formation of the completely *N*-de-methylated dye. Besides, the methyl groups are removed one by one as confirmed by the gradual wavelength shifts of the maximum-peaks toward the blue region. The hypsochromic effects resulting from *N*-de-methylated and hydroxylated intermediates of the CV dye occurred concomitantly during irradiation. The reaction mechanisms of TiO_2/UV proposed in this study would shed some light for future application of the technology for decoloration of dyes.

References

[1] Triarylmethane and diarylmethane dyes. In: Ullmann's encyclopedia of industrial chemistry. 6th ed., vol. A27. New York: Wiley-VCH; 2001.

[2] Pagga U, Bruan D. Chemosphere 1986;15:479.
[3] Reife A. Dyes, environmental chemistry. In: Kirk, editor. Kirk-Othmer encyclopedia of chemical technology. 4th ed., vol. 8. New York: John Wiley & Sons, Inc; 1993. p. 753.
[4] Coopper P. Asian Text J 1995;3:52.
[5] Azmi W, Sani RK, Banerjee UC. Enzyme Microb Technol 1998;22:185.
[6] Watanabe N, Horikoshi S, Kawasaki A, Hidaka H, Serpone N. Environ Sci Technol 2005;39:2320.
[7] Chen CC, Zhao W, Li JG, Zhao JC, Hidaka H, Serpone N. Environ Sci Technol 2002;36:3604.
[8] Parra S, Stanca SE, Guasaquillo I, Thampi KR. Appl Catal B Environ 2004;51:107.
[9] Asahi R, Morikawa T, Ohwaki T, Aoki K, Taga Y. Science 2001;293:269.
[10] Bouzaida I, Ferronato C, Chovelon JM, Rammah ME, Herrmann JM. J Photochem Photobiol A Chem 2004;168:23.
[11] Karkmaz M, Puzenat E, Guillard C, Herrmann JM. Appl Catal B Environ 2004;51:183.
[12] Kyung H, Lee J, Choi W. Environ Sci Technol 2005;39:2376.
[13] Hidaka H, Honjo H, Horikoshi S, Serpone N. New J Chem 2003;27:1371.
[14] Yang Y, Guo Y, Hu C, Wang Y, Wang E. Appl Catal A Gen 2004;273:201.
[15] Měšťánková H, Krýsa J, Jirkovský J, Mailhot G, Bolte M. Appl Catal B Environ 2005;58:185.
[16] Lu P, Wu F, Deng NS. Appl Catal B Environ 2004;53:87.
[17] Chen CC, Li X, Zhau J, Hidaka H, Serpone N. J Phys Chem B 2002;106:318.
[18] Linsebigler AL, Lu GQ, JTY Jr . Chem Rev 1995;95:735.
[19] Wang R, Hashimoto K, Fujishima A, Chikuni M, Kojima E, Kitamura A, et al. Nature 1997;388:431.
[20] Zou Z, Ye J, Sayama K, Arakawa H. Nature 2001;414:625.
[21] Hoffman MR, Martin ST, Choi W, Bahnemann W. Chem Rev 1995;95:69.
[22] Zollinger H. In: Color chemistry: syntheses, properties, and applications of organic dyes and pigments. 2nd ed. Weinheim: VCH; 1991.
[23] Feller RL. Accelerated aging. Photochemical and thermal aspects. The J. Paul Getty Trust; 1994.
[24] <http://members.pgonline.com/~bryand/StainsFile/>.
[25] Baptista MS, Indig GL. J Phys Chem B 1998;102:4678.
[26] Kowaltowski AJ, Turin J, Indig GL. J Bioenerg Biomembr 1999;31:581.
[27] Bhasikuttan AC, Sapre AV, Shastri LV. J Photochem Photobiol A Chem 2002;150:59.
[28] Lewis LM, Indig GL. J Photochem Photobiol B Biol 2002;67:139.
[29] Bonnett R, Martinez G. Tetrahedron 2001;57:9513.
[30] Kanela K, Bartlett JA, Indig GL. Photochem Photobiol Sci 2002;1:309.
[31] Cho BP, Yang T, Blankenship LR, Moody JD, Churchwell M, Bebland FA, et al. Chem Res Toxicol 2003;16:285.
[32] Doerge DR, Chang HC, Divi RL, Churchwell MI. Chem Res Toxicol 1998;11:1098.
[33] Saquib M, Muneer M. Dyes Pigments 2003;56:37.
[34] Li X, Liu G, Zhao J. New J Chem 1999;23:1193.
[35] Zhao J, Hidaka H, Takamura A, Pelizzetti E, Serpone N. Langmuir 1993;9:1646.
[36] Boehm HP. Discuss Faraday Soc 1971;52:264.
[37] Ohtani B, Okugawa Y, Nishimoto S, Kagiya T. J Phys Chem 1987;91:3550.
[38] Kim DH, Anderson MA. J Photochem Photobiol A Chem 1996;94:221.
[39] Wu T, Liu G, Zhao J, Hidaka H, Serpone N. J Phys Chem B 1998;102:5845.
[40] Zhao J, Wu T, Wu K, Oikawa K, Hidaka H, Serpone N. Environ Sci Technol 1998;32:2394.
[41] Liu G, Li X, Zhao J, Hidaka H, Serpone N. Environ Sci Technol 2000;34:3982.
[42] Kerr GH, Meth-Cohn O. J Chem Soc C 1971;1369.
[43] Galliani G, Rindone B, Scolastico C. Tetrahedron Lett 1975;1285.
[44] Shaefer FC, Zimmermann WD. J Org Chem 1970;35:2165.
[45] Laube BL, Asirvatham MR, Mann CK. J Org Chem 1977;42:670.
[46] Wu T, Lin J, Zhao J, Hidaka H, Serpone N. Environ Sci Technol 1999;33:1379.
[47] Liu G, Wu T, Zhao J, Wu K, Oikawa K, Hidaka H, et al. New J Chem 2000;24:411.
[48] Liu G, Zhao J, Wu K, Oikawa K, Hidaka H, et al. Environ Sci Technol 1999;33:2081.